

Avionics-Based GNSS Integrity Augmentation Performance in a Jamming Environment

Roberto Sabatini¹, Terry Moore², Chris Hill² and Subramanian Ramasamy¹

¹School of Aerospace, Mechanical and Manufacturing Engineering
RMIT University, Melbourne, VIC 3000, Australia

²Nottingham Geospatial Institute
University of Nottingham, NG7 2TU, UK

Abstract

Intentional and unintentional radiofrequency interference (i.e., jamming) can result in degraded navigation accuracy or complete loss of the GNSS signal tracking. Jammers can be classified into three broad categories: Narrowband Jammers (NBJ), Spread Spectrum Jammers (SSJ) and Wideband Gaussian Jammers (WGJ). In recent years, a number of effective jamming detection and anti-jamming (filtering and suppression) techniques have been developed for military GNSS applications and some of them are envisaged to be used for civil purposes (e.g., terrorist attacks). The synergies between these jamming detection techniques and our newly developed Avionics-Based Integrity Augmentation (ABIA) system are investigated in this paper. In particular, GNSS vulnerability to NBJ, SSJ and WGJ types of jamming is analytically described in terms of Jamming to Signal (J/S) tracking thresholds and the models for calculating the minimum acceptable aircraft-to-jammer ranges are presented. Simulation results demonstrate that the proposed ABIA architecture is capable of performing jamming detection and avoidance when GNSS is considered as the primary source of navigation data.

Keywords: Global Navigation Satellite System, Jamming, Air Navigation, Integrity Augmentation and Trajectory Optimisation.

Introduction

Typically, GNSS signals reach the airborne receivers at very low power, and radiofrequency interference can be the result of a number of potential sources including:

- Unintentional interference in the operating frequency band.
- Intentional jamming (e.g., premeditated GNSS signal attack including terrorist activities and electronic warfare).
- High-power signals in the adjacent frequency bands.
- Denial of service and scheduled outages.
- Natural interference including solar flares.

The positioning accuracy obtained from the satellite signals is degraded or completely lost due to jamming and in turn affects the availability of the system. The current reliance on GNSS signals for many safety- and mission-critical tasks raises the issue of electronic warfare vulnerability and at the same time safety of other aircraft. Jamming tolerance can be increased with smarter processing techniques in the receiver prior to the detection stage. Furthermore, the spectral spreading techniques adopted in GNSS receivers mitigate the effect of jamming. Although the GPS system is well designed to mitigate any jamming effects, like any radio receiver, it can still be jammed. Anti-jamming techniques become essential once the signal strength of the interfering signal becomes significant. Considering a sample case of Global

Positioning System (GPS) signals, the L1 C/A signal received from the 25 W transmitter with a 13 dBiC antenna at a range of 12, 550 miles is in the order of -150 dBW. The impact caused by jamming on GNSS detection capability has been studied and analytically described [1, 2]. Though a number of effective jamming detection and anti-jamming (filtering and suppression) techniques have been developed in the last two decades for military applications, only a few methods are available for civil use [3, 4]. A number of systems have been designed and implemented to detect jamming such as Jammer Detection and LOcation System (JLOC) in the US and GNSS Availability, Accuracy, Reliability and Integrity Assessment for timing and Navigation system (GAARDIAN) in UK. Jammers are classified into three broad categories: Narrowband Jammers (NBJ), Spread Spectrum Jammers (SSJ) and Wideband Gaussian Jammers (WGJ). Typical jamming signals can be classified into four classes:

- Class I: continuous wave signal.
- Class II: chirp signal with one saw-tooth function.
- Class III: chirp signal with multi saw-tooth functions.
- Class IV: chirp signal with frequency bursts.

In the majority of cases, jamming signals are transmitted in the L1/E1 band, which are used in receivers for civilian applications. These signals can affect all GNSS signals including GPS, Galileo, GLObalnaya NAvigatsionnaya Sputnikovaya Sistema (GLONASS), BeiDou (Compass), Indian Regional Navigational Satellite System (IRNSS) and Quasi-Zenith Satellite System (QZSS).

ABIA System

In the case of an avionics navigation system, integrity directly relates to the level of confidence that can be placed in the information provided by the on-board system. It includes the ability of the navigation system to provide timely and valid warnings to users when the system must not be used for the intended operation or phase of flight. Specifically, an avionics navigation system is required to deliver an alert of any malfunction (as a result of a set alert threshold being exceeded) to users within a given period of time. The GNSS augmentation is based on additional information provided by other avionic systems. In most cases, the additional avionic systems operate via separate principles than the GNSS and, therefore, are not subject to the same sources of error or interference. A system such as this is referred to as an Avionics-Based or Aircraft-Based Augmentation System (ABAS). While other available augmentation systems such as Ground Based Augmentation System (GBAS) and Satellite-Based Augmentation System (SBAS) address all GNSS performance augmentation including accuracy, integrity, availability and continuity, the ABAS approach is particularly significant to increase the levels of integrity and accuracy of GNSS in a variety of mission- and safety-critical aviation applications. Previous research on Avionics-Based Integrity Augmentation (ABIA) demonstrated the potential of this technology to enhance GNSS integrity performance in a variety of mission- and safety-critical applications including experimental flight test/flight inspection, precision approach and autoland [5-7]. An advanced ABIA integration scheme was also developed specifically addressing the cooperative and non-cooperative Sense-and-Avoid (SAA) functions required in Remotely Piloted Aircraft Systems (RPAS) applications [8]. The ABIA system architecture is illustrated in Fig. 1. The on-board sensors provide information on the aircraft relevant flight parameters to an Integrity Flag Generator (IFG). Using the available data on GNSS and the relevant aircraft flight parameters, integrity signals are generated which are transmitted to the cockpit display and also provided as aural warnings to the pilots. These integrity flags are subsequently used by a Flight Path Optimisation Module (FPOM). The ABIA system addresses both the predictive and reactive nature of GNSS integrity augmentation by producing suitable integrity flags (cautions and warnings) in

case of predicted/ascertained GNSS data losses or unacceptable signal degradations exceeding the Required Navigation Performance (RNP) specified for each phase of flight. Additionally, it provides information to the on-board pilot in a manned aircraft or to the RPAS pilot in the Ground Control Station (GCS) to avoid further data losses/degradations.

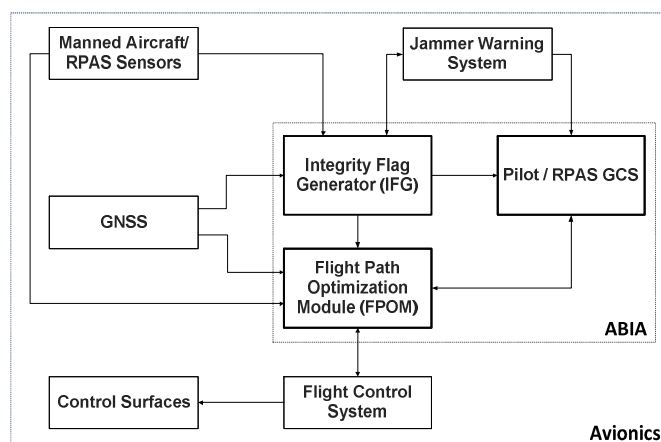


Fig. 1: ABIA system architecture. Adapted from [8].

The IFG module generates the Caution Integrity Flag (CIF) and Warning Integrity Flag (WIF) alerts. The CIF is a predictive annunciation that the GNSS data delivered to the avionics system is going to exceed the RNP thresholds specified for the current and planned flight operational tasks (GNSS alert status), while the WIF is a reactive annunciation that the GNSS data delivered to the avionics system has exceeded the RNP thresholds specified for the current flight operational task (GNSS fault status). The Time-to-Caution (TTC) is defined as the minimum time allowed for the caution flag to be provided to the user before the onset of a GNSS fault resulting in an unsafe condition and Time-to-Warning (TTW) is the maximum time allowed from the moment a GNSS fault resulting in an unsafe condition is detected to the moment that the ABIA system provides a warning flag to the user.

ABIA Integrity Flags for Jamming

The main causes of GNSS data degradation or signal losses in aviation applications are analytically modeled in [5, 6]. The threshold limits required for the IFG to produce caution and warning flags are identified in [7]. The thresholds are set based on the aircraft-satellite relative geometry including estimated Horizontal and Vertical Position Error (HPE/VPE), radio frequency elements and receiver tracking loops. The Scalar Tracking Loops (STL) typically employs Delay Lock Loops (DLL) to track the code phase and Phase Lock Loops (PLL) or Frequency Lock Loops (FLL) to track the carrier phase. Current state-of-the-art STL also employ combined PLL and FLL for carrier tracking to obtain better results in navigation position accuracy and to enhance tracking [5-8]. Currently, Vector Tracking Loops (VTL) are also employed, which are based on advanced receiver architectures capable of tracking signals in a combined manner [9]. VTL provide the advantages of operating at a lower total carrier power to noise ratio (C/N_0) and in higher dynamics environments when compare with STL logics. A typical GNSS receiver is connected to a GNSS antenna and consists of a RF front end, a digital signal processor used to calculate code range, carrier phase and Doppler frequencies and to generate the navigational data, and a navigation processor used to calculate the Position, Velocity and Time (PVT) solution. The method adopted to determine the CIF and WIF thresholds are described in [5, 6]. The link budget of the direct GNSS signals received by the aircraft in the presence of atmospheric propagation disturbances is calculated

based on C/N_0 , as well as the applicable radiofrequency interference. In general, the effects of GNSS signal jamming are:

- Jamming affects the GNSS receiver's C/N_0 .
- Signal-to-noise ratio (S/N) decreases.
- Jamming contributes to multipath effects of GNSS signals in dense urban areas.
- When jamming exists, GNSS receivers might react differently from the ideal case.

The relationship between effective carrier-to-noise ratio (C/N) and jammer signal power (J) is given by [10]:

$$\frac{C}{N} = [C/N_0] / \left[1 + \frac{(\frac{C}{N_0})(\frac{J}{S})}{R_c} \right] \quad (1)$$

where N_0 is the thermal noise power spectral density, R_c is the P-code chipping rate, S is the signal power received at the GNSS antenna input, C is the carrier power and J/S is the jamming-to-signal ratio. In the general method, range to the jammer, atmospheric losses, and a corresponding noise in the jammer are computed, all as a function of time along the trajectory. Jamming is modelled based on the J/S levels. The J/S performance of a GNSS receiver at its tracking threshold can be evaluated by the following equation [11]:

$$\frac{J}{S} = 10 \log Q R_c \left[1/10^{0.1(\frac{C}{N_0})_{MIN}} - 1/10^{0.1(\frac{C}{N_0})} \right] \quad (2)$$

where Q is the processing gain adjustment factor and is equal to 1 for Narrowband Jammers (NBj), 1.5 for Spread Spectrum Jammers (SSj) and 2 for Wideband Gaussian Jammers (WGj), R_c is the code chipping rate (chips/s) and $(C/N_0)_{MIN}$ is the receiver tracking threshold (dB-Hz). Since the weak limit in an avionics receiver is the carrier tracking loop threshold, this threshold is usually substituted for $(C/N_0)_{MIN}$. During the flight test activities performed on TORNADO-IDS with unaided C/A code avionics receivers, it was found that in all dynamics conditions explored and in the absence of jamming, a (C/N_0) of 25 dB-Hz was sufficient to keep tracking the satellites. As an example, using this 25 dB-Hz tracking threshold, we can calculate the J/S performance of the TORNADO-IDS GPS receiver considering one of the satellites tracked during the descent and during this manoeuvre, the C/N_0 for Pseudo Random Noise (PRN) PRN-14 was about 37 dB-Hz. Table 1 shows the corresponding J/S calculations, assuming $(C/N_0)_{MIN} = 25$ dB-Hz.

Table 1: J/S calculations for 25 dB-Hz tracking threshold

Jamming	Q	R_c	$(C/N_0)_{threshold}$	(C/N_0)	J/S
NBJ	1	$1.023 * 10^6$	25 dB-Hz	37	34.82
SSJ	1.5	$1.023 * 10^6$	25 dB-Hz	37	36.58
WGJ	2	$1.023 * 10^6$	25 dB-Hz	37	37.83

The transmitted power of the jammer and its distance with respect to the GNSS receiver required for jamming is expressed in terms of Effective Radiated Power (ERP). Using these J/S values, the minimum range in metres from a jamming source can be calculated from:

$$R_{min} = \frac{\lambda_j}{4\pi} 10^{\frac{ERP_{tj} - P_{rj} + G_{rj} - L_{rf}}{20}} \quad (3)$$

where ERP_{tj} is the effective radiated power of the jammer (dBw), λ_j is the wavelength of jammer frequency (m), P_{rj} is the received (incident) jamming power level at threshold = $J/S + P_{rs}$ (dBw), P_{rs} is the minimum received (incident) signal power (dBw), G_{rj} is the GNSS

antenna gain towards the jammer (dBiC) and L_{rf} is the jammer power attenuation due to recover front-end filtering (dB). The PLL, FLL and DLL error models described in [6] allow determining the C/N_0 corresponding to the receiver tracking thresholds. The integrity flag criterion applicable to the ABIA system is [7, 8]:

$$\left(\frac{C}{N_0}\right)_{Threshold} = \max \left[\left(\frac{C}{N_0}\right)_{PLL}, \left(\frac{C}{N_0}\right)_{FLL}, \left(\frac{C}{N_0}\right)_{DLL}, \left(\frac{C}{N_0}\right)_{PLL+FLL}, \left(\frac{C}{N_0}\right)_{VTL} \right] \quad (4)$$

where $(C/N_0)_{PLL}$ is the minimum C/N_0 for PLL tracking, $(C/N_0)_{FLL}$ is the minimum C/N_0 for FLL tracking, $(C/N_0)_{DLL}$ is the minimum C/N_0 for DLL tracking, $(C/N_0)_{PLL+FLL}$ is the minimum C/N_0 for combined PLL and FLL tracking and $(C/N_0)_{VTL}$ is the minimum C/N_0 for VTL based tracking. In general, when the PLL loop order is made higher, there is an improvement in dynamic stress performance. Therefore, third order PLL are widely adopted in avionics GNSS receivers. Assuming 15 to 18 Hz noise bandwidth and 5 to 20 msec pre detection integration time (typical values for avionics receivers), the tracking threshold for the PLL gives 25 to 28 dB-Hz. The main error associated with a GNSS receiver FLL are the dynamics stress error and frequency jitter caused due to thermal noise. The receiver tracking threshold is adopted such that the 3-sigma jitter must not exceed one-fourth of the frequency pull-in range of the FLL discriminator. Using theoretical and experimental threshold values, the receiver J/S performance for the various cases of practical interest are calculated. When available, flight test data collected in representative portions of the aircraft operational flight envelope shall be used. The criteria for generating CIF and WIF based on J/N ratio is described in earlier research [5-7, 11-12]. Considering an additional 5% margin on the 3-sigma tracking thresholds for the CIF, the following detailed criteria are introduced for the ABIA integrity thresholds:

- When either $42.25^\circ \leq 3\sigma_{PLL} \leq 45^\circ$ or $0.2375T \leq 3\sigma_{FLL} \leq 0.25T$ or $0.05d \leq 3\sigma_{DLL} \leq d$, the CIF shall be generated.
- When either $3\sigma_{PLL} > 45^\circ$ or $3\sigma_{FLL} > 1/4T$ or $3\sigma_{DLL} > d$, the WIF shall be generated.

The processing of GNSS signals in a receiver specific to anti-jamming function is illustrated in Fig. 2. Interference detection is typically performed based on a number of receiver parameters including output power, variance and standard deviation of the output power (correlated), carrier phase uncertainty and Automatic Gain Control (AGC) values. The key component to detect interference in the received signal is the Automatic Gain Control (AGC). In order to minimize the signal loss, the amplitude of the received GNSS signal is tuned to the ADC range. The gain in AGC drops significantly when there is an increased power in the GNSS bandwidth. The chirp signals are predominantly used for jamming in the recent times. Chirp signals are typically sinusoidal or cosine signals with sweeping of frequency within in-band GNSS frequency ranges. The chirp signals are modelled using a periodic Frequency Modulated (FM) signal and can be expressed as [12, 13]:

$$x(t) = a \sin(2\pi \sum_{h=0}^{\infty} (\int_0^t f_1(t' - h.T_{s,1}).dt' + \dots + \int_0^t f_n(t' - h.T_{s,n}).dt')) \quad (5)$$

where $f_1(t' - h.T_{s,1})$ is the 1st saw tooth function, $f_n(t' - h.T_{s,n})$ is the nth saw tooth function, $T_{s,n}$ is the sweep time. A number of algorithms have been proposed for jamming detection, localisation and characterisation of interfering signals. Considering a GNSS jammer transmitting chirp signals (with zero mean) from a random position, the received signal can be expressed as:

$$s_r(t) = s_t(t) \sqrt{\left(\frac{c}{f_c \cdot 4\pi \cdot d}\right)^\alpha} \cdot e^{j2\pi f_c d/c} \quad (6)$$

where $s_t(t)$ is the transmitted jammer signal, f_c is the carrier signal, d is the distance between the jammer and the receiver, α is the path loss and c is the speed of light. In order to improve the hostile effects of GNSS in electronic warfare and terrorist attacks, new generation signals

are being introduced. These signals inherently possess higher precision of orientation and anti-jamming performance, and are also compatible existing GNSS signals. Binary Offset Carrier (BOC) modulation is introduced to increase the ERP for anti-jamming performance without affecting the existing GNSS signals. In these cases, Costas loop is used as carrier tracking loop to receive BOC modulated signals. When a jamming signal interferes with the GNSS signal, phase measurement error increases beyond a specified threshold value and as a consequence the tracking loop loses lock.

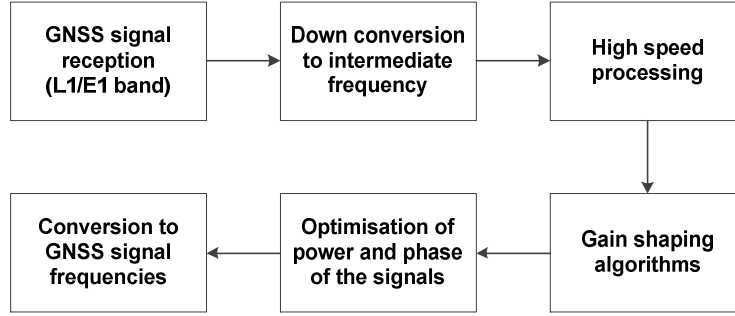


Fig. 2: GNSS receiver processing for anti-jamming function

The design of the GNSS antenna generally provides a superior polarisation signal reception and poor low elevation angle gain. As a result of superior polarisation, cross polarisation reception is less than -10dBic and thus effectively reduces unwanted signal reflections. In order to design GNSS receivers against interference, bandwidth, sampling and hardware considerations are taken into account. In order to increase the accuracy of the signal, narrow correlator spacing is employed by sharpening up the auto correlation function. Therefore, it is ensured that the correlators are still operating in a linear range. Noise increases due to the increase in pre-correlation bandwidth but it can effectively tackled by employing superior digital signal processing algorithms. Generally, the signal processor adopted has the capability of performing code correlation in two different modes: an early-minus-late power mode and a dot-product mode. The signal processor has two correlators in each channel and can operate one of the correlators as an early or an early-minus-late correlator. The normalised dot-product discriminator is given by [14]:

$$d\tau = \frac{I_{e-I}I_P + Q_{e-I}Q_P}{I_P^2 + Q_P^2} \quad (7)$$

where I and Q values are summed over the Prediction Integration Interval (PDI). I_{e-I} and Q_{e-I} represent the I and Q values when the hardware is implemented in the dot-product mode. P stands for I and Q and are similar to the ones used in carrier loop discriminators. For an infinite pre-correlation bandwidth, the normalised Early-minus-Late (EL) discriminator has an output at high values of SNR and the estimation is given by:

$$E(d\tau) = \frac{4(2-d)\tau}{(2-d)^2 + 4\tau^2} \text{ chips, } -d/2 \leq \tau \leq d/2 \quad (8)$$

where τ is the tracking error and d is the EL discriminator spacing in chips. The standard deviation of the pseudorange observations (σ_τ) is estimated from the discriminator output standard deviation (σ_d) and is given by:

$$\sigma_\tau = \frac{\sqrt{2TB}}{G_d} \sigma_d \quad (9)$$

where G_d is the gain of the discriminator and B is the bandwidth. For example, for a loop bandwidth of 1/30 Hz, the resulting σ_τ is approximately 0.3 cycles. In avionics receivers, lock detectors are used to assess if the satellite signals are being tracked or not tracked. Code lock detection is adopted, which is very similar to estimating the received C/N₀, inferring that the

receiver is operating on or near the correlation peak. The code-correlation process of the receiver is designed to increase the signal strength when compared to that of inherent and added noise. The spread spectrum processing gain (G_p) is defined as the ratio of the spread bandwidth to the unspread (baseband) bandwidth and is expressed in dB. The post-correlation S/N is given as:

$$(S/N)_{post-corr.} = (S/N)_{pre-corr.} + G_p \quad (10)$$

When the receiver code is aligned with the transmitted code, the signal power at the band pass output is crushed into approximately 100 Hz of bandwidth. The processing gain can be calculated from:

$$G_p = 10 \log \left(\frac{2C_R}{T_D} \right) [dB] \quad (11)$$

where C_R is the chipping rate and T_D is the data period. For the C/A code this works out to be about 43 dB. Typical avionics receivers have a cut off value at 10 dB, which means that if the value is less than this the satellite signal level is too low to be used in the positioning computations [14]. An additional threshold criterion to be accounted for in the ABIA system is given as:

$$S/N_{post-corr.} = S/N_{pre-corr.} + G_p \geq 10 \text{ dB} \quad (12)$$

- When G_p is more than 11 dB (margin of 1 dB), the CIF shall be generated.
- When G_p is less than 9 dB (margin of 1 dB), the WIF shall be generated.

Avoidance of Jamming Environment

A number of jamming mitigation techniques are normally adopted as counteract measures. The adoption of filters to fade out the jamming signal is usually employed. Specifically, a notch filter (narrowband band stop filter) is used against continuous wave or narrowband electronic attacks. Selective Availability Anti-Spoofing Modules (SAASM) are employed by the US DoD for tackling spoofing of GNSS signals. Controlled Radiation Pattern Antenna (CPRA) offering null steering is often bulky and expensive. Multi-constellation / multi-frequency receivers including the ones using embedded Software Defined Radio (SDR) based processing are used for tackling jamming. An analysis of the identified degradation results in inferring that a common criterion based on satellite elevation variation in the body frame can be adopted. Depending upon the technique used to capture the jammer's coordinates, the targeting error represents approximately half of the final Circular Error Probable (CEP). Earlier methods to overcome jamming adopted the integration of GNSS with other navigation sensors; say Inertial Navigation System (INS) sensors [10]. When it is detected that the tracking loop (PLL/FLL/DLL/VTL) has lost lock in a jamming environment, the GNSS signal is decoupled from the integrated navigation system and then guidance for avoidance trajectory is obtained from the calibrated INS operating in a coast mode. Generally, in a tightly coupled architecture, the GNSS data is used to aid the navigation solution, and the INS is used to remove the majority of the error from the signal input to the GPS tracking loops. The amount of Doppler error that can be removed is determined from the accuracy of the navigation solution, and further, by the dynamics of the manned aircraft/RPAS. If the integrated navigation solution is more accurate, then the error is drastically reduced and the receiver loop bandwidth is reduced leading to the susceptibility to jammer noise. The GPS carrier tracking loop is more susceptible to jamming due to the small wavelength of the carrier (0.19 metres) compared to the P-code chip width (29.3 meters). One method of detecting carrier loop lock is to monitor the detected phase error estimate (u) in the PLL and is expressed as [10]:

$$\text{Track quality indicator} = \cos 2u \quad (13)$$

The threshold of the loop is dynamically altered according to the computed S/N ratio and it is assumed that a loss of lock is evident when the signal strength falls below a fixed threshold. In order to compute the signal generated for input to the tracking loops, noise due to both thermal and jammer sources is superimposed on the signals. Noise is generally assumed to be Gaussian in nature and its power is obtained from C/N value and the noise power is given by:

$$\text{Noise power} = P_s B / (C/N) \quad (14)$$

where P_s is the received satellite signal power and B is the prediction bandwidth. The design of avoiding jamming environment by adopting ABIA system involves the evaluation of the overall avoidance volume. The overall avoidance volume is obtained by combining the avoidance volume resulting from the jammer and uncertainty volume resulting from positional deviations. Extended Kalman Filter (EKF), Unscented Kalman Filter (UKF) or particle filter is used for multi-sensor data fusion of different navigation sensors to obtain the Position, Velocity and Attitude (PVA) estimates. Pseudo-spectral optimisation (PSO) or constrained Differential Geometric Optimization (DGO) techniques are used to generate the new trajectory based on the available time to conflict (host manned aircraft/RPAS entering the jamming avoidance volume). The shape of the combined jamming avoidance volume and navigation errors is described using spherical harmonics. Depending on if the errors are statistically independent or dependent; the resultant volume is obtained for uncorrelated or correlated errors respectively [16-19]. The selection of the optimal trajectory from the generated set of safe trajectories is based on minimisation of the following cost function:

$$J = w_t \cdot t_{SAFE} + w_f \int [SFC \cdot T(t)] dt - w_d \cdot D_{min} - w_{id} \cdot \int D(t) dt \quad (15)$$

where $D(t)$ is the estimated distance of the generated avoidance trajectory points from the avoidance volume associated with the obstacle, $D_{min} = \min[D(t)]$ is the estimated minimum distance of the avoidance trajectory from the avoidance volume, $t_{SAFE} = t|_{D_{min}}$ is the time at which the safe avoidance condition is successfully attained, $SFC \left[\frac{kg}{N} \cdot s \right]$ is the specific fuel consumption, $T(t)$ is the thrust profile, and w_t, w_f, w_d, w_{id} are the weightings attributed to time, fuel, distance and integral distance respectively. In time-critical avoidance applications (i.e., closing-up on jamming environments at high relative velocities especially for military aircraft) appropriate higher weightings are used for the time and distance cost elements. Based on the criteria identified for integrity monitoring and augmentation, the jamming environment represented by the radiation pattern is avoided by initiating avoidance manoeuvres obtained from the FPOM. In order to constrain the trajectory optimization process, dynamic constraint criteria are adopted.

Simulation Cases

Simulation case studies to evaluate the performance of the proposed GNSS ABIA integrity augmentation strategy were performed in a number of test platforms (3-DoF and 6-DoF aircraft dynamics models) including AIRBUS 320 (A320), TORNADO-IDS and AEROSONDE RPAS. In all scenarios including multipath environments [15], an overall avoidance volume is generated based on the SAA Unified Method (SUM) proposed in [19]. An avoidance trajectory is generated based on the available time to conflict using PSO or DGO techniques. Time and fuel are used in the cost functional, the aircraft dynamics model produces the dynamics constraints, and the satellite elevation criteria are used to set path constraints for both PSO and DGO techniques [5]. Based on the obtained position uncertainty about the host manned aircraft or RPAS trajectory, an optimised avoidance trajectory without any GNSS data losses is constructed around the overall avoidance volume obtained by combining the jamming signal radiation pattern and navigation error of the host platform. The optimised avoidance trajectory is constructed tangential to the radiation pattern of the jammer

(main lobe in the case of directional jammer). The optimised avoidance trajectory obtained in the presence of directional and non-directional jammers is illustrated in Fig. 5 and 6 respectively.

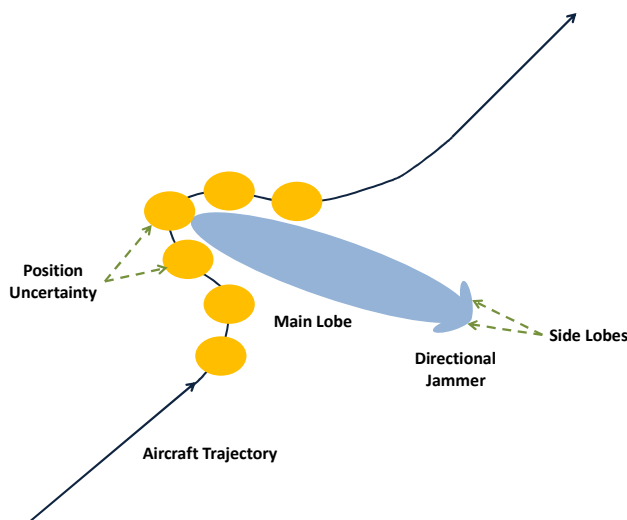


Fig.5: Optimised avoidance trajectory in the presence of directional jammer

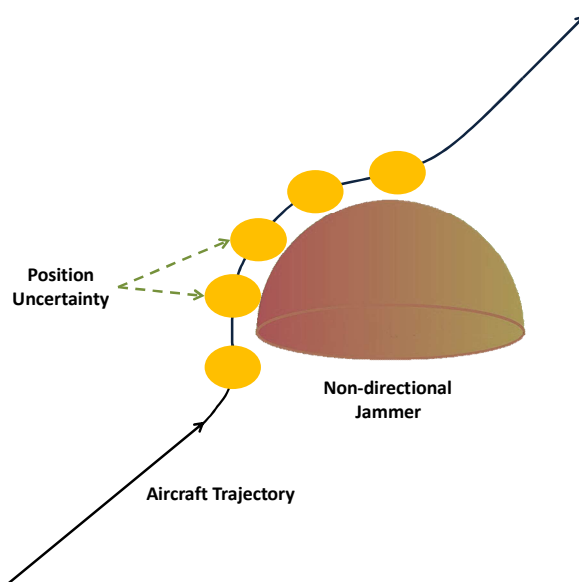


Fig.6: Optimised avoidance trajectory in the presence of non-directional jammer

A simulation run performed in MATLABTM and Simulink for the directional jammer case is also illustrated in Fig. 7. The AEROSONDE RPAS 6-DoF dynamics model was used for this simulation run. After the conflict detection and resolution was determined with respect to the jamming radiation pattern, the avoidance trajectory was generated and optimized based on the cost function defined earlier. Additionally, the constraints imposed by ABIA in terms of RPAS platform dynamics and GNSS constellation satellite elevation angles were considered to generate the optimised avoidance trajectory and thus preventing degradation or losses of navigation data during the whole jammer avoidance loop.

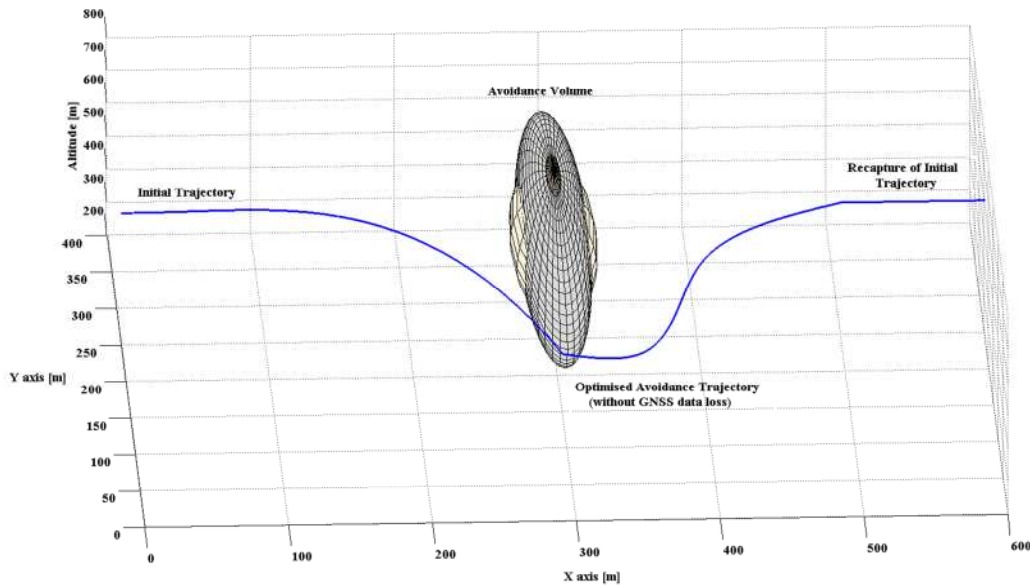


Fig.7: Trajectory in the presence of directional jammer

Conclusion

In this research the effects of jamming on GNSS integrity augmentation performance were examined. The analytical models of Jamming-to-Signal (J/S) tracking thresholds for different types of jamming were described. In particular, the models for calculating the minimum acceptable aircraft-to-jammer ranges and the determination of the overall avoidance volume were presented. Simulation case studies conducted in the presence of directional and non-directional jammers demonstrated the capability of the on-board ABIA system to avoid jamming. Further research is focussing on the ABIA evolutions for Next Generation Flight Management System (NG-FMS) applications [20-23] as well as trajectory optimization for future CNS+A systems and 4 Dimensional Trajectory (4DT) Intent Based Operations (IBO).

References

1. Ndili, A. and Enge, D.P., "GPS receiver autonomous interference detection", *Proceedings of the IEEE Position, Location and Navigation Symposium—PLANS 98*, Palm Spring, CA, USA 1998.
2. Landry, R.J., Calmetes, V. and Bousquet, M., "Impact of interference on a generic GPS receiver and assessment of mitigation techniques", *Proceedings of the IEEE 5th International Symposium on Spread Spectrum Techniques and Applications Proceedings*, Vol. 1, 1998, pp. 87–91.
3. Landry, R.J., René, Boutin P. and Constantinescu, A., "New anti-jamming technique for GPS and GALILEO receivers using adaptive FADP filter", *Digital Signal Processing*, Vol. 16, No. 3, 2006, pp. 255-274.
4. Ward, P., "GPS Receiver RF Interference Monitoring, Mitigation, and Analysis Techniques", *NAVIGATION, Journal of the Institute of Navigation*, Vol. 41, No. 4 (Winter), pp. 367-391, 1994-95.
5. Sabatini, R., Moore, T. and Hill, C., "Avionics-Based GNSS Integrity Augmentation for Unmanned Aerial Systems Sense-and-Avoid", *Proceedings of the 26th International Technical Meeting of the Satellite Division of the Institute of Navigation: ION GNSS+ 2014*, Tampa, Florida, USA, 2014.

6. Sabatini, R., Moore, T. and Hill, C., "A New Avionics Based GNSS Integrity Augmentation System: Part 1 – Fundamentals", *Journal of Navigation*, Vol. 66, No. 3, May 2013, pp. 363-383. DOI: 10.1017/S0373463313000027
7. Sabatini, R., Moore, T. and Hill, C., "A New Avionics Based GNSS Integrity Augmentation System: Part 2 – Integrity Flags", *Journal of Navigation*, Vol. 66, No. 4, June 2013, pp. 511-522. DOI: 10.1017/S0373463313000143
8. Sabatini, R., Moore, T. and Hill, C., "GNSS Avionics-Based Integrity Augmentation for RPAS Detect-and-Avoid Applications", *Proceedings of the Fourth Australasian Unmanned Systems Conference*, December 2014. DOI: 10.13140/2.1.3268.5120
9. Kiesel, S., Ascher, C., Gramm, D. and Trommer, G.F., "GNSS Receiver with Vector based FLL-assisted PLL Carrier Tracking Loop", *Proceedings of the 21st International Technical Meeting of the Satellite Division of The Institute of Navigation (ION GNSS 2008)*, Savannah, GA, USA, 2008.
10. Kessler, K.M., Karkalik, F.G. and Sun, J., "Performance Analysis of Integrated GPS/INS Guidance for Air-to-Ground Weapons in a Jamming Environment", *Proceedings of the Fourth International Technical Meeting of the Satellite Division of The Institute of Navigation, ION GPS*, pp. 139-148, September 1991.
11. Kaplan E.D. and Hegarty, C.J., "Understanding GPS: Principles and Applications", Artech House, Second Edition, 2006, pp. 197-203.
12. Bartolucci, M., Casile, R., Corazza, G.E., Durante, A., Gabelli, G. and Guidotti, A., "Cooperative/distributed Localization and Characterization of GNSS Jamming Interference", *Proceedings of the 2013 International Conference on Localization and GNSS (ICL-GNSS)*, 2013, pp. 1-6.
13. Liang, G.B., Li, F., Zhang, X.H. and Chen, Y., "Characteristic and Anti-jamming Performance of New Generation GNSS Signals", *Proceedings of the IEEE 14th International Conference on Communication Technology (ICCT)*, 2012, pp. 622-628.
14. Fenton, P.C., Falkenberg, W.H., Ford, T.J. and Ng, K.K., "NovAtel's GPS Receiver – The High Performance OEM Sensor of the Future", *Proceedings of the Fourth International Technical Meeting of the Satellite Division of The Institute of Navigation, ION GPS*, pp. 49-58, September 1991.
15. Braasch, M.S., "On the Characterization of Multipath Errors in Satellite-based Precision Approach and Landing Systems", College of Engineering and Technology, Ohio University, June 1992.
16. Ramasamy, S., Sabatini R. and Gardi, A., "Avionics Sensor Fusion for Small Size Unmanned Aircraft Sense-and-Avoid", *Proceedings of the IEEE Workshop on Metrology for Aerospace*, Benevento, Italy, May 2014, pp. 271-276. DOI: 10.1109/MetroAeroSpace.2014.6865933
17. Rodriguez, L., Sabatini, R., Gardi A. and Ramasamy, S., "A Novel System for Non-Cooperative UAV Sense-and-Avoid", *Proceedings of the European Navigation Conference 2013*, Vienna, Austria, April 2013.
18. Sabatini, R., Gardi, A. and Ramasamy, S., "A Laser Obstacle Detection and Avoidance System for Unmanned Aircraft Sense-and-Avoid", *Applied Mechanics and Materials*, Vol. 629, Trans Tech Publications, Switzerland, 2014, pp. 355-360. DOI: 10.4028/www.scientific.net/AMM.629.355
19. Ramasamy, S., Sabatini, R. and Gardi, A., "Towards a Unified Approach to Cooperative and Non-Cooperative RPAS Detect-and-Avoid", *Proceedings of the Fourth Australasian Unmanned Systems Conference 2014 (ACUS 2014)*, Melbourne, Australia. DOI: 10.13140/2.1.4841.3764

20. Sabatini, R., Liu, Y., Ridder, K. De., Gardi, A., Ramasamy, S., Zammit-Mangion D. and Rodriguez, L., "ENDEAVOUR Project – Novel Avionics and ATM Systems for SESAR and NextGen", *Proceedings of the Avionics Europe 2013 – Tackling the Challenges in Avionics: Single Sky Many Platforms*, Munich, Germany, February 2013.
21. Ramasamy, S., Sabatini, R., Gardi A. and Kistan, T., "Next Generation Flight Management System for Real-Time Trajectory Based Operations", *Applied Mechanics and Materials*, Vol. 629, Trans Tech Publications, Switzerland, 2014, pp. 344-349. DOI:10.4028/www.scientific.net/AMM.629.344
22. Ramasamy, S., Sangam, M., Sabatini R. and Gardi, A., "Flight Management System for Unmanned Reusable Space Vehicle Atmospheric and Re-entry Trajectory Optimisation", *Applied Mechanics and Materials*, Vol. 629, Trans Tech Publications, Switzerland, 2014, pp. 304-309. DOI: 10.4028/www.scientific.net/AMM.629.304
23. Gardi, A., Sabatini, R., Ramasamy S. and Kistan, T., "Real-Time Trajectory Optimisation Models for Next Generation Air Traffic Management Systems", *Applied Mechanics and Materials*, Vol. 629, Trans Tech Publications, Switzerland, 2014, pp. 327-332. DOI: 10.4028/www.scientific.net/AMM.629.327